JOURNAL OF BIOMEDICAL OPTICS 4(1), 36–46 (JANUARY 1999)

OPTICAL PROPERTIES OF CIRCULATING HUMAN BLOOD IN THE WAVELENGTH RANGE 400–2500 NM

André Roggan,[†] Moritz Friebel,[‡] Klaus Dörschel,[†] Andreas Hahn,[*] and Gerhard Müller[†,‡]
[†]Institut für Medizinische/Technische Physik und Lasermedizin, Universitätsklinikum Benjamin Franklin, Freie Universität Berlin, Krahmerstr. 6-10, D-12207 Berlin, Germany; [‡]Laser- und Medizin-Technologie gGmbH, Berlin, Germany; [*]Stöckert Instrumente GmbH, München, Germany

(Paper ODB-007 received Dec. 29, 1997; manuscript accepted for publication Nov. 6, 1998.)

ABSTRACT

Knowledge about the optical properties μ_a, μ_s, and g of human blood plays an important role for many diagnostic and therapeutic applications in laser medicine and medical diagnostics. They strongly depend on physiological parameters such as oxygen saturation, osmolarity, flow conditions, haematocrit, etc. The integrating sphere technique and inverse Monte Carlo simulations were applied to measure μ_a, μ_s, and g of circulating human blood. At 633 nm the optical properties of human blood with a haematocrit of 10% and an oxygen saturation of 98% were found to be $0.210 \pm 0.002\,\mathrm{mm}^{-1}$ for μ_a, $77.3 \pm 0.5\,\mathrm{mm}^{-1}$ for μ_s, and 0.994 ± 0.001 for the g factor. An increase of the haematocrit up to 50% lead to a linear increase of absorption and reduced scattering. Variations in osmolarity and wall shear rate led to changes of all three parameters while variations in the oxygen saturation only led to a significant change of the absorption coefficient. A spectrum of all three parameters was measured in the wavelength range 400–2500 nm for oxygenated and deoxygenated blood, showing that blood absorption followed the absorption behavior of haemoglobin and water. The scattering coefficient decreased for wavelengths above 500 nm with approximately $\lambda^{-1.7}$; the g factor was higher than 0.9 over the whole wavelength range. © *1999 Society of Photo-Optical Instrumentation Engineers.*
[S1083-3668(99)00501-8]

Keywords blood; optical properties; extracorporal circulation; absorption; scattering; phase function.

1 INTRODUCTION

As given by transport theory, the optical parameters are defined by the absorption coefficient μ_a in mm^{-1}, the scattering coefficient μ_s in mm^{-1} and the mean cosine of the scattering angle g (anisotropy factor) in combination with a scattering phase function $p(\mathbf{s},\mathbf{s}')$.[1,2] Knowledge about the optical parameters of blood plays an important role for many diagnostic and therapeutic applications in laser medicine and medical routine diagnosis. To calculate the light distribution in blood perfused tissues, knowledge about the optical properties of blood is required for a number of optical methods, such as optical tomography, optical biopsy, diaphanoscopy, photodynamic therapy, laser induced thermotherapy, or portwine stains and haemangioma treatment. Normal human whole blood consists of about 55 vol % plasma (90% water, 10% proteins) and 45 vol % cells (99% red blood cells ''erythrocytes,'' 1% leukocytes and thrombocytes). A red blood cell (RBC) has a characteristic flat biconcave form with a diameter of 7 to 8 μm and a thickness of 2 μm (Figure 1). The RBC has a mean volume of 90 $\mu\mathrm{m}^3$ and contains 30 pg haemoglobin that allows oxygen transport. The cell concentration in blood under physiological conditions is approximately $5 \times 10^{12}\ \mathrm{L}^{-1}$.

However, only few theoretical and experimental studies about the optical properties of blood have led to reasonable results because the optical properties of blood mainly depend on physiological and biochemical parameters such as haematocrit, flow, osmolarity, haemolysis, and oxygen saturation. Haematocrit (hct) is the volume fraction of cells within the whole blood volume and ranges from 36.8% to 49.2% under physiological conditions. The haemoglobin concentration ranges from 134 to 173 g/L for whole blood and from 299 to 357 g/L for RBCs. Flow induced shear stress can influence phenomena such as sedimentation, reversible agglomeration, axial migration or cell deformation, and orientation. The flow parameters depend on the blood viscosity and they are influenced by the fact that blood is not a Newton fluid. A change in osmolarity induces a variation of the RBC volume due to water exchange and therefore has an impact on the haemoglobin concentration within the RBC. Haemolysis is coupled with the damage of RBC membranes by mechanical or chemical impact with

Address all correspondence to André Roggan, PhD. Tel: 49-30-8449-2327; Fax: 49-30-8449-2399; E-mail: A.Roggan@Lmtb.de

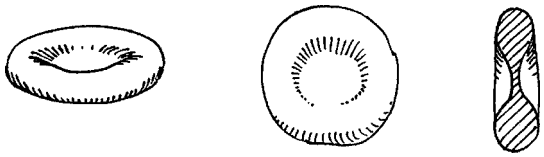

Fig. 1 Human erythrocyte.

consecutive release of haemoglobin into the plasma. Finally, oxygenation of haemoglobin leads to characteristic changes in its absorbing behavior. This effect is used in clinically available blood oxymeters.

All mentioned parameters have to be precisely controlled during optical measurements and the blood has to be kept moving to avoid sedimentation and clustering. A physiological flow is correlated with a shear rate of approximately 500 s^{-1} in the capillary system. Therefore an experimental setup was realized to provide measurements of the optical blood properties in the wavelength range 400–2500 nm under flow conditions using a specially designed flow cuvette in combination with an extracorporal circulation and oxygenation unit.

2 MATERIAL AND METHODS

2.1 BLOOD PREPARATION

Fresh erythrocyte concentrates from human donors were centrifuged three times and washed in phosphate buffer solution (300 mosmol/L, *p*H 7.4). By doing this the blood samples contained no plasma proteins, leukocytes, or thrombocytes. Light microscopy control of the samples ensured that they were neither haemolysed nor were the cells deformed. The haematocrit (hct) was used as a measure for the concentration of red blood cells and was adjusted by dilution with phosphate buffer. Blood samples were investigated with a haematocrit value between 2.5% and 70%. Dilution with buffers of different osmolarities allowed the adjustment of various blood osmolarities from 225 to 450 mosmol/L. In addition, a quantitative haemolysis was induced by diluting one part of the blood sample with distilled water, readjusting the osmolarity to 300 mosmol/L by adding buffer solution, and mixing the haemolyzed sample with the intact blood sample. Blood circulation and predetermined oxygen states were adjusted with an extracorporal circulation unit (Stöckert Instrument GmbH, Germany). The blood was gently stirred and kept flowing through a specially designed turbulence free cuvette with a laminar flow and an optical path of 97 μm (Figure 2). Oxygen saturation was adjusted by continuous flow of a mixture of O_2, N_2, and CO_2 through a modified membrane oxygenator. The oxygen saturation was continuously controlled by a blood oxymeter (OxySAT-Meter SM 0200; Baxter). For complete deoxygenation the erythrocyte concentrates were diluted with phosphate buffer containing 0.3% sodium dithionite ($Na_2S_2O_4$). With the

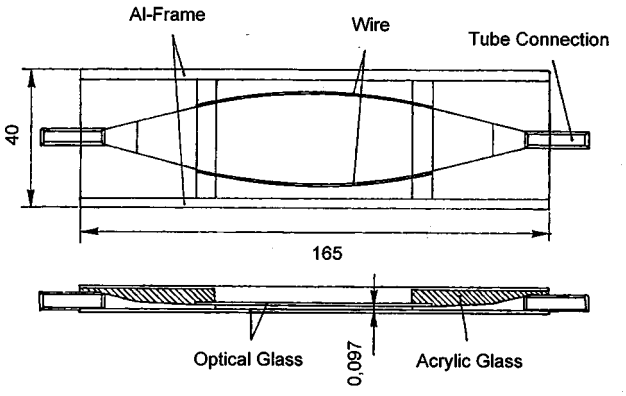

Fig. 2 Turbulence free flow cuvette with a thickness of 97 μm.

exception of experiments based on changing oxygen states, all investigations were derived with an oxygen saturation over 98%. The blood temperature was kept constant at 20 °C.

2.2 EXPERIMENTAL SETUP

The optical properties of scattering and absorbing media cannot be measured directly. As a result, the optical blood properties were determined by a double integrating sphere technique, evaluating the diffuse backscattering R_d, the total transmission T_t, and the collimated, i.e., nonscattered, transmission T_c of thin samples (Figure 3).[3–6] The inner surfaces of the integrating spheres (∅152 mm) were coated with a highly reflecting layer of Spectralon®, allowing the total radiation in the hemispheres in front and behind the sample to be collected. Reflection standards were used to calibrate the system (Labsphere). All measurements with respect to

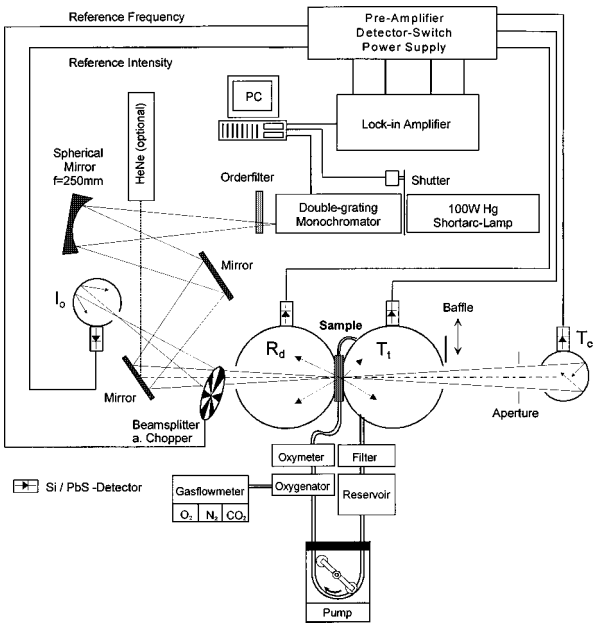

Fig. 3 Experimental setup for the determination of optical properties of human blood (Refs. 4–6).

varying physiological blood parameters were carried out at a fixed wavelength of 632.8 nm, using a helium–neon laser with 1.2 mW output power (Spindler & Hoyer). The spot size in the sample plane was ∅7 mm; the distance between sample and T_c detector was 1330 mm; The aperture in front of the T_c detector was ∅5 mm, the beam diameter in the aperture plane was ∅1.2 mm. A mercury high pressure short arc lamp served as light source for the spectral overview of optical properties (Osram, 100 W, 2×10^6 cd/cm^2). The lamp was connected to a monochromator (AMKO, $f=200$ mm) with a resolution of 8 nm [full width at half maximum (FWHM)] in the range 400–1140 nm and 16 nm (FWHM) in the range 1140–2500 nm. The circular monochromator exit slit (∅1 mm) was focused on the flow cuvette, providing a spot size of ∅4 mm. The distance between sample and T_c detector was 430 mm, the aperture in front of the T_c detector was ∅30 mm, and the beam diameter in the aperture plane was ∅25 mm. The beam was mechanically chopped at 220 s^{-1} and part of the beam was used for the reference intensity compensation. Silicon photodiodes (AMKO, 09-SiU04-C, 400–1140 nm) and lead sulphide photodiodes (AMKO, 09-Pb01-C, 1140–2500 nm) were used as detectors. The signals were finally recorded with a lock-in technique (ITHACO 3981).

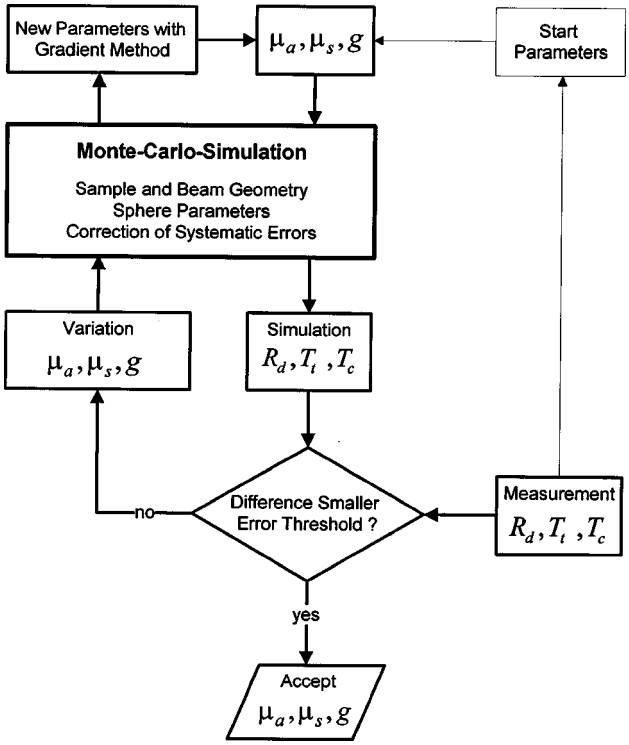

Fig. 4 Scheme of the inverse Monte Carlo simulation for the calculation of optical properties from measured data (Refs. 4–6).

2.3 EVALUATION OF OPTICAL PROPERTIES

The extraction of the optical parameters μ_a, μ_s, and g from the measurements is a complex task as there are no analytical models available with sufficient precision. The method of choice was therefore the Monte Carlo simulation, which as a statistical method calculates the trajectories of a great number of photons (3×10^5 in our experiments) and as a result presents the remission and transmission characteristics of a sample for a given set of optical parameters. In order to solve the opposite situation, i.e., to determine the unknown optical parameters from the measured macroscopic values, the Monte Carlo simulation had to be inverted[4–6] (Figure 4). For this the measured data were simulated taking an estimated set of start parameters μ_a, μ_s, and g from Kubelka–Munk theory.[7] Then the measured quantities were calculated and compared with the real measurements. In case of a significant deviation all three parameters were varied slightly and three new forward simulations were performed. After this procedure a gradient matrix was built up, allowing the calculation of new optical parameters which fit better to the measured quantities. This procedure was repeated until the deviation between measured and calculated values was within the error threshold (fixed to 0.1%). Thus the associated set of optical parameters could be accepted. As well as a high degree of accuracy, the method offered a simple means of compensating systematic errors such as radiation losses, scattered photons detected at the T_c detector, deviations from a Lambertian distribution of the diffuse reflectance, and an incomplete separation of the radiation fields in the integrating spheres. The potential disadvantage of long calculation times was compensated for by the use of currently available fast computer systems.

One of the most important questions when dealing with Monte Carlo simulations of photon transport in turbid media is the choice of a scattering phase function that fits best to the investigated medium. Therefore the Henyey–Greenstein phase function was most often used in biomedical optics because of its good correspondence to goniophotometric measurements of tissues like skin or parenchymatous organs:[8–17]

$$p_{\mathrm{HG}}(\mathbf{s},\mathbf{s}') = \frac{1-g_{\mathrm{HG}}^2}{4\pi(1+g_{\mathrm{HG}}^2-2g_{\mathrm{HG}}\cos\Theta)^{3/2}}.$$

Here $p_{\mathrm{HG}}(\mathbf{s},\mathbf{s}')$ is the normalized probability for a photon to be scattered from a direction $\mathbf{s}$ into a direction $\mathbf{s}'$, and g_{HG} is the free parameter which equals the mean cosine of the scattering angle, known as the anisotropy factor g. On the other hand, it is known that the Henyey–Greenstein phase function does not fit to the scattering of RBCs because of their large diameter. Hence Yaroslavsky proposed the Gegenbauer–Kernel phase function for blood samples.[18] This is a two parameter function with $\alpha_{\mathrm{GK}}>0$ and $-1\leqslant g_{\mathrm{GK}}\leqslant 1$. The Gegenbauer–Kernel phase function equals the

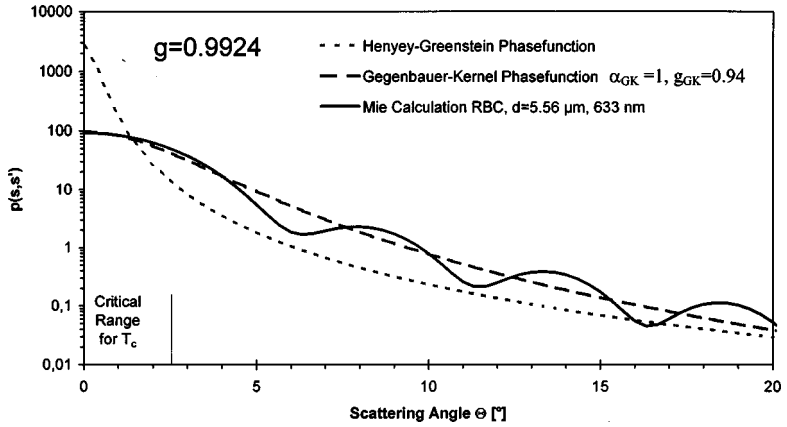

Fig. 5 Comparison of various phase functions for red blood cells.

Henyey–Greenstein phase function for $\alpha_{GK}=0.5$. The anisotropy factor g has to be calculated numerically:

$$p_{GK}(\mathbf{s},\mathbf{s}') = \frac{\alpha_{GK} g_{GK}}{\pi((1+g_{GK})^{2\alpha_{GK}} - (1-g_{GK})^{2\alpha_{GK}})} \times \frac{(1-g_{GK}^2)^{2\alpha_{GK}}}{(1+g_{GK}^2 - 2g_{GK}\cos\Theta)^{\alpha_{GK}+1}}.$$

The importance of a correct phase function becomes evident with regard to photons which travel through the measuring cuvette and which are scattered only once or twice. These photons have a high probability to be collected in the T_c detector because of the extreme forward scattering of RBCs. Thus these photons had to be considered as a T_c offset in the Monte Carlo routine, but the amount of this offset strongly depended on the selected phase function. This is shown in Figure 5 where three phase functions with the same anisotropy factor of $g=0.9924$ were compared. Mie calculations of the RBC phase function at 633 nm served as a reference where a mean diameter of 5.56 μm was selected as a spherical RBC equivalent with a volume of 90 μm^3. The refractive index was set to $n=1.333$ for the surrounding medium and to $n=1.402$ for the RBC. That the Mie calculation for a spherical equivalent is a valid assumption for RBCs could be shown in the subsequent measurements at various plasma osmolarities (see Secs. 3.3 and 3.4 for detailed information). Evidently the Henyey–Greenstein phase function overestimates the RBC phase function by a factor of approximately 30 within the first degrees of the scattering angle that are critical for the T_c detection. On the other hand, the Gegenbauer–Kernel phase function with $\alpha_{GK}=1.0$ mimics the Mie function without significant deviations in the critical range. Therefore the Gegenbauer–Kernel phase function was implemented in the Monte Carlo model and a fixed factor of $\alpha_{GK}=1$ was applied for all subsequent evaluations while the factor g_{GK} was the free fit parameter. The anisotropy factor g was finally calculated numerically from α_{GK} and g_{GK}.

2.4 EXECUTION OF MEASUREMENTS

For each experimental question a total of three independent measurement series were carried out using erythrocyte concentrates from different human donors. One measurement series at a fixed wavelength of 633 nm with varying haematocrit, shear rate, osmolarity, haemolysis, or oxygenation required approximately 60 min. The evaluation of the optical properties applying inverse Monte Carlo simulations required a total time of 10–20 h for all three series of one experiment. Mean values and standard deviations were calculated as shown in the subsequent graphs. The spectral overview required approximately 5 h for each spectrum which was also measured three times in order to calculate mean values of optical properties. Before and after each measurement the blood samples were checked for their haematocrit as well as for possible haemolysis and cell deformation.

3 RESULTS AND DISCUSSION

3.1 HAEMATOCRIT

Isotonic blood samples (300 mosmol/L) of various haematocrits were measured at a wavelength of 633 nm. Figure 6 shows the mean values ($n=3$) of μ_a, μ_s, g, and μ_s' depending on the haematocrit ranging from 0% to 70% at a constant shear rate of 500 s^{-1}. The absorption coefficient μ_a increased linearly with the haematocrit over the whole measured haematocrit range. The scattering coefficient μ_s also increased proportionally to the haematocrit but only for values of hct$\leqslant$10%. The anisotropy factor g was almost constant in that haematocrit range ($0.994 > g > 0.992$). On the other hand, μ_s appeared to be independent of blood concentration at values hct $>$10% and the g factor decreased continuously

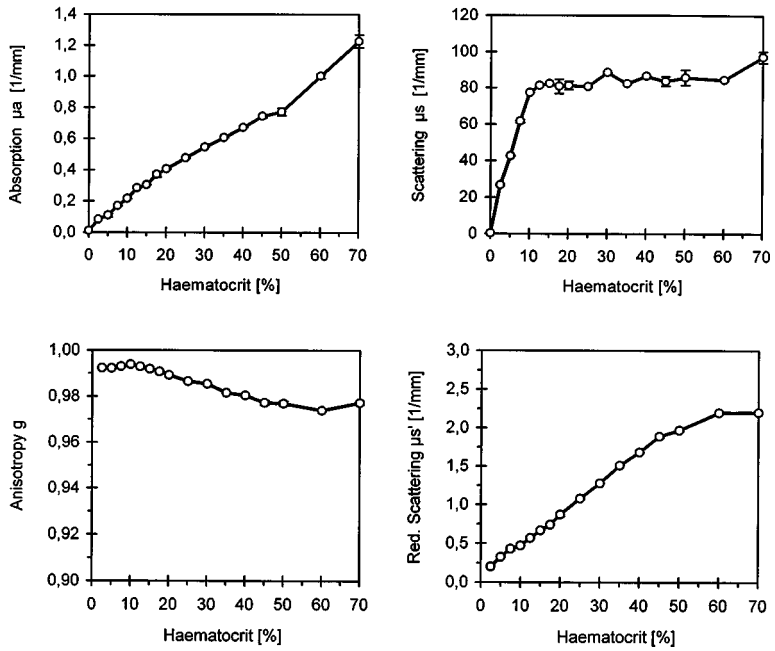

Fig. 6 Mean values ± SD ($n=3$) of μ_a, μ_s, g, and μ_s' vs haematocrit ($\pi=300$ mosmol/L, $\gamma=500\ s^{-1}$, $SatO_2>98\%$, $\lambda=633$ nm).

down to 0.975 at hct 70%. One could conclude from investigation of the measured quantities that the collimated transmission dropped below the detection threshold for hct>10%. Therefore the calculation of three independent optical properties was not possible at high hct levels and consequently the reduced scattering coefficient $\mu_s'=\mu_s(1-g)$ was evaluated. In contrast to μ_s a linear increase was found for μ_s' up to hct 45%. Above 45% a slight saturation effect was found which might be the result of either interfering scattering events or the formation of RBC clusters. This nonlinear scattering dependence on haematocrit was already predicted by Reynolds from theoretical investigations.[19] Due to the incomplete separation of μ_s and g only μ_s' was calculated for blood samples at haematocrits above 10%.

3.2 FLOW VELOCITY

The optical properties were measured under various flow conditions to derive the effects of blood flow on μ_a and μ_s' (Figure 7). The underlying mechanism for cell deformation and axial migration was the predominating shear force within the flow cuvette. Therefore the shear rate was calculated from the ratio of flow velocity and cuvette cross section. The range of the adjusted shear rate corresponded to the physiological range in the human vascular system. A low shear rate of 50 s^{-1} led to a decrease of μ_a to 95% compared to a short flow stop. Additional increase of the shear rate resulted in a continuous but smaller decrease of μ_a down to 88% at $\gamma=3000\ s^{-1}$. The reduced scattering coefficient μ_s' showed a similar behavior with increasing shear rates. μ_s' decreased to 93% at $\gamma=50\ s^{-1}$ and to 80% at $\gamma=3000\ s^{-1}$. It could be clearly shown that the flow velocity and the related shear rates had a significant impact on the optical properties of blood. However, from the measured data it was not possible to differentiate if the shear rate dependence was a result of cell deformation or axial mi-

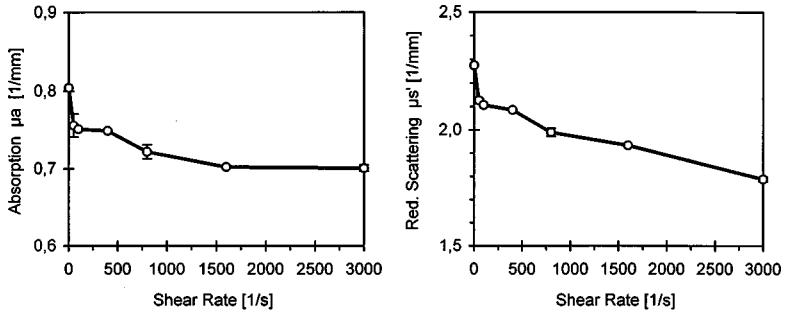

Fig. 7 Mean values ± SD ($n=3$) of μ_a and μ_s' vs shear rate (hct=41%, $\pi=300$ mosmol/L, $\gamma=500\ s^{-1}$, $SatO_2>98\%$, $\lambda=633$ nm).

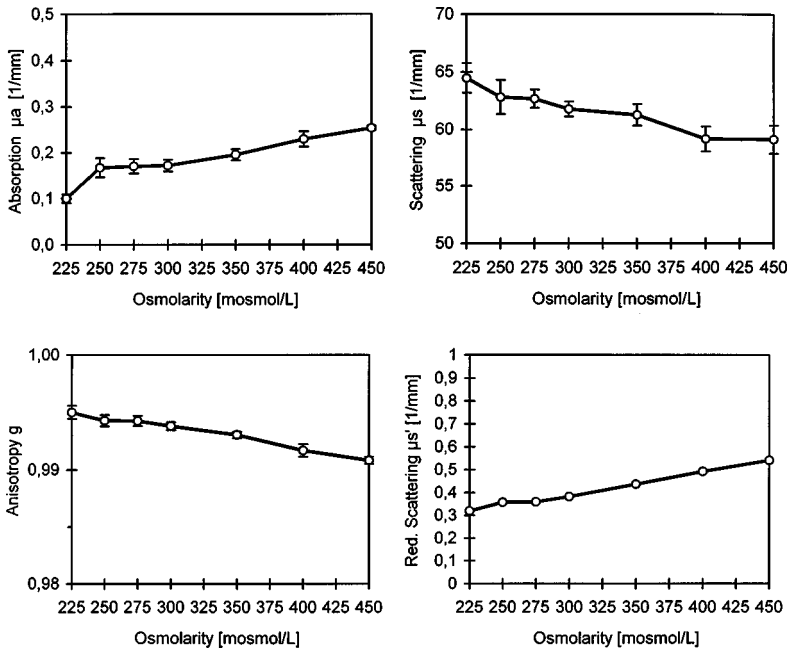

Fig. 8 Mean values ± SD ($n=3$) of μ_a, μ_s, μ_s', and g at short flow stop vs plasma osmolarity (hct=7.5% at 300 mosmol/L, $\gamma = 0\ s^{-1}$, $SatO_2>98\%$, $\lambda = 633$ nm).

gration. Thus, further measurements with different geometrical shapes of RBC were carried out by varying the osmolarity of the buffer.

3.3 OSMOLARITY

Variation in the plasma osmolarity led to considerable changes in the shape of the erythrocytes. Hyperosmotic plasma induces cell shrinking (acanthocytes); in hypo-osmotic plasma the cells swell (spherocytes). In both cases deformability of the erythrocyte is distinctly diminished. Diluted blood samples (hct=7.5% at 300 mosmol/L) were adjusted to osmolarity values ranging from 225 to 450 mosmol/L using phosphate buffer solutions of various osmolarity. Because the number of cells per volume was kept constant for these experiments, the haematocrit varied slightly with osmolarity due to the different cell volumes. Figure 8 shows the measured optical properties at a wavelength of 633 nm.

The absorption coefficient μ_a increased continuously with osmolarity, i.e., cell shrinkage led to an increase of μ_a. At 225 mosmol/L μ_a amounted to 60% of the value measured under isotonic conditions while μ_a was 50% above the isotonic value at 450 mosmol/L. This effect was unexpected because the number of cells, and therefore the overall concentration of absorbing haemoglobin, was kept constant during all measurements with different osmolarities. An explanation will be given in the discussion of the measurements on haemolysed blood samples. The scattering coefficient μ_s showed a slight decrease with increasing osmolarity of about 10%. Also the anisotropy factor g decreased from 0.995 at 225 mosmol/L down to 0.991 at 450 mosmol/L. The reduced scattering coefficient μ_s' increased linearly with osmolarity. In contrast to the absorption properties, the scattering behavior appeared to be reasonable because the cell shape and the refractive index of the cell bounded haemoglobin solution varied with osmolarity, both strongly affecting the scattering performance.

Mie calculations on red blood cells were carried out applying the algorithms of Zijp and ten Bosch[20] to differentiate between the impact of cell shape and refractive index. Therefore the cell shape was assumed to be spherical when applying Mie theory and the sphere diameter was adjusted to mimic the RBC volume coupled to a certain osmolarity. The refractive index of the cell bounded haemoglobin solution was derived by the equation $n_{\text{solution}} = n_{\text{water}} + \beta \cdot c$, where c is the haemoglobin concentration in g/100 ml and $\beta = 0.001\,942$ at a wavelength of 589 nm.[21] Assuming a mean erythrocyte volume of 90 μm^3 and an inner cell haemoglobin concentration of 350 g/L (35 g/100 ml) for isotonic conditions, a refractive index of $n_{300}=1.402$ and a sphere equivalent diameter of $d_{300}=5.56$ μm were calculated. Considering slight variations of the haematocrit at 250 mosmol/L (hct 8.1%, RBC volume 96.7 μm^3, RBC haemoglobin concentration 325 g/L) and 400 mosmol/L (hct 6.6%, RBC volume 78.6 μm^3, RBC haemoglobin concentration 400 g/L) the corresponding refractive indices were $n_{250}=1.397$ and $n_{400}=1.412$ and the sphere equivalent diameters were $d_{250}=5.70$ μm and $d_{400}=5.32$ μm. The scattering coefficients were calculated by multiplying the Mie scattering cross section with the num-

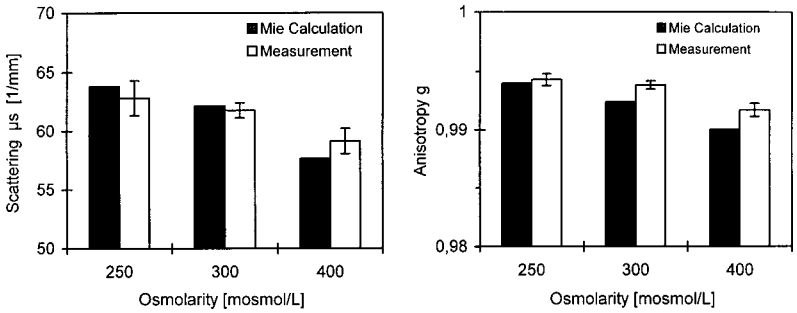

Fig. 9 Measured mean values ± SD ($n=3$) of μ_s and g compared with Mie calculations for spherical equivalents (hct=7.5% at 300 mosmol/L, $\gamma=0\ s^{-1}$, $SatO_2>98\%$, $\lambda=633$ nm).

ber density of $8.33\times10^{11}\ L^{-1}$ which was related to hct=7.5% at 300 mosmol/L and which was kept constant at all osmolarities.

Figure 9 shows the results of the Mie calculations for μ_s and g compared with the measured data. At 250 mosmol/L μ_s were calculated to be 63.8 mm^{-1} vs $62.8\pm1.5\ mm^{-1}$ for the measured value, at 300 mosmol/L 62.2 mm^{-1} vs $61.8\pm0.7\ mm^{-1}$ and 57.7 mm^{-1} vs $59.1\pm1.1\ mm^{-1}$ at 400 mosmol/L. The calculated values of g were 0.994 vs 0.9943 ± 0.0005 at 250 mosmol/L, 0.9924 vs 0.9938 ± 0.0004 under isotonic conditions and 0.990 vs 0.9917 ± 0.0006 at 400 mosmol/L. The agreement of measurements and calculations indicated that the shape of the erythrocytes was of minor importance for the scattering properties of blood. Variations in the scattering behavior were due to changes in cell volume and refractive index. In addition, these results showed that the dependence of the absorption and scattering behavior on shear rate was mainly caused by a dynamic decrease of haematocrit as a result of axial migration (Fahraeus effect), while shear stress induced cell deformation could be neglected with respect to the optical properties.

3.4 HAEMOLYSIS

Blood samples of different haemolytic states were prepared by mixing intact and completely haemolyzed blood without removing the membrane residuals. Figure 10 shows the measured optical properties at five different degrees of haemolysis between 0% and 100%.

The absorption coefficient μ_a significantly decreased with increasing haemolysis. When blood was completely haemolyzed, μ_a amounted to $0.11\pm0.03\ mm^{-1}$ which was only 55% of the value for intact blood ($0.20\pm0.05\ mm^{-1}$). Nevertheless, the dependence of haemoglobin absorption on haemolysis rate was as unexpected as the increase of absorption with increasing osmolarity because

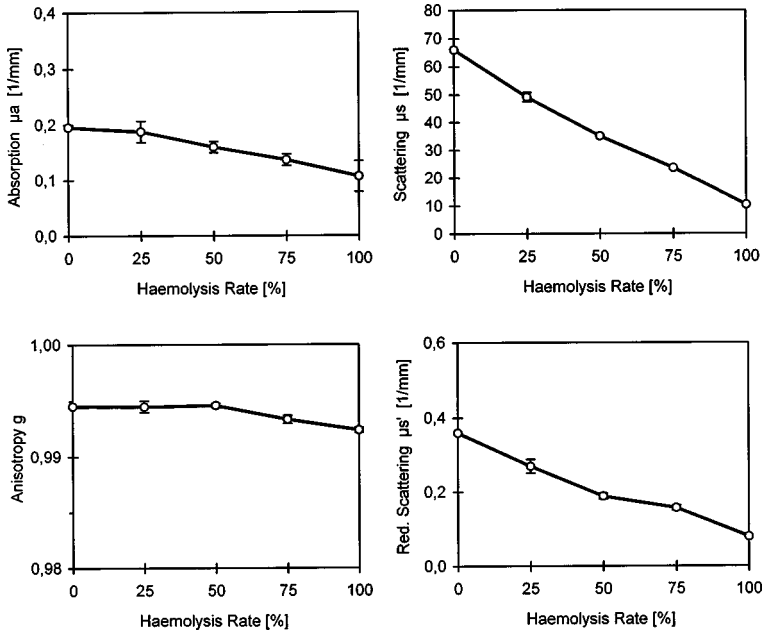

Fig. 10 Mean values ± SD ($n=3$) of μ_a, μ_s, g, and μ_s' vs extent of haemolysis (hct=7.5%, $\pi=300$ mosmol/L, $\gamma=500\ s^{-1}$, $SatO_2>98\%$, $\lambda=633$ nm).

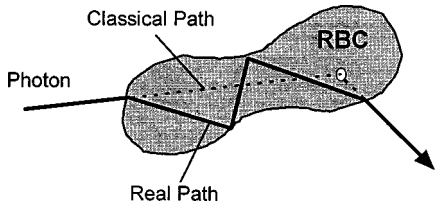

Fig. 11 Path of a photon within an erythrocyte.

the overall haemoglobin concentration was kept constant. The fact that absorption was higher in blood than in a haemoglobin solution with the same concentration was also found by comparing literature data and scaling the reported absorption coefficients to our concentration of 27 g/L (hct =7.5%). For an oxygenated haemoglobin solution Gordy,[22] Steinke,[23] and Kuenstner[24] reported a mean μ_a of $0.064 \pm 0.013\ \mathrm{mm}^{-1}$ at 633 nm. On the other hand, Reynolds[19] and Steinke[25] reported a mean μ_a of $0.12 \pm 0.04\ \mathrm{mm}^{-1}$ for whole human blood. The values were slightly smaller than our data but the same factor of approximately two could be deduced.

The scattering coefficient μ_s showed a distinct decrease with increasing haemolysis. At complete haemolysis μ_s amounted to 18% of the value measured for intact blood. The anisotropy factor g was constant up to 50% haemolysis and slightly decreased at higher haemolysis rates. μ_s' decreased continuously, reaching values of about 16% compared to intact blood. The decrease of scattering with increasing haemolysis rate followed from the fact that destroyed erythrocytes distributed their haemoglobin into the whole solution, resulting in a refractive index match. Thus the RBCs loose their scattering properties. Consequently the measurements showed that the residual erythrocyte membranes have only a minor impact on the scattering properties that might be understood from their very small wall thickness of about 4 nm.

Even more remarkable was the significant decrease in absorption when blood was haemolyzed or osmolarity was decreased. This phenomenon found an explanation in the special scattering and absorbing structure of blood. Here scattering cannot be assumed to occur at point scatterers with absorption taking place in the surrounding (nonscattering) medium. In blood the scatterers themselves have a significant dimension compared to the whole volume and they contain all or at least part of the absorbers. Hence it has to be taken into consideration that the optical path of a photon within a scatterer might be increased due to multiple reflections at its internal boundary (Figure 11). This effect of internal reflections is well known from atmospherical scattering in water drops and is responsible for the occurrence of rainbows. The increased pathlength on its part leads to a higher absorption probability of the whole solution if absorbers are contained within the scatterers. Consequently, this resulted in a decrease of the overall absorption coefficient if more erythrocytes loose their scattering properties due to haemolysis. The described phenomenon also explains the increase of μ_a if osmolarity increases (see Figure 8). Here the RBC refractive index increased due to the higher RBC haemoglobin concentration in the hyperosmolar state. Hence the number of internal reflections also increased, resulting in a higher total absorption coefficient. Nonlinear absorption aspects as a concentration dependent extinction coefficient and the ''Sieve'' effect can be excluded to describe the results because they would reduce μ_a with increasing inner cell haemoglobin concentration and not vice versa.

3.5 OXYGEN SATURATION

To elucidate the influence of oxygen saturation on the optical properties of blood a sample (hct 41%) was investigated at different oxygen saturations between 100% and 30%, adjusted by insufflation of N_2 and CO_2. Figure 12 shows the measured values of μ_a and μ_s' versus O_2 saturation. At a wavelength of 633 nm μ_a showed a linear decrease with increasing O_2 saturation. Completely oxygenated blood showed approximately half the absorption of blood with an oxygen saturation of 30%. The reduced scattering coefficient μ_s' remained constant over the measured range of oxygen saturation. As was ex-

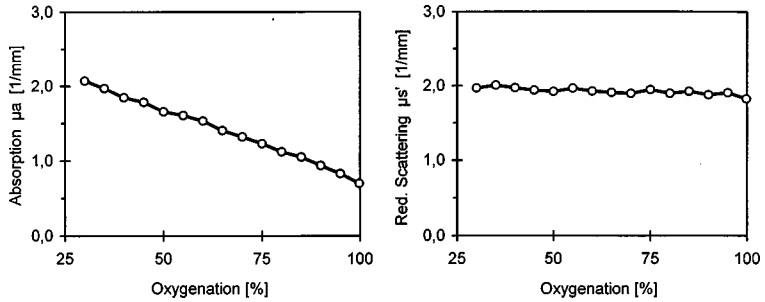

Fig. 12 Absorption coefficient μ_a and reduced scattering coefficient μ_s' vs O_2 saturation (hct=41%, π=300 mosmol/L, $\gamma=500\ \mathrm{s}^{-1}$, λ =633 nm).

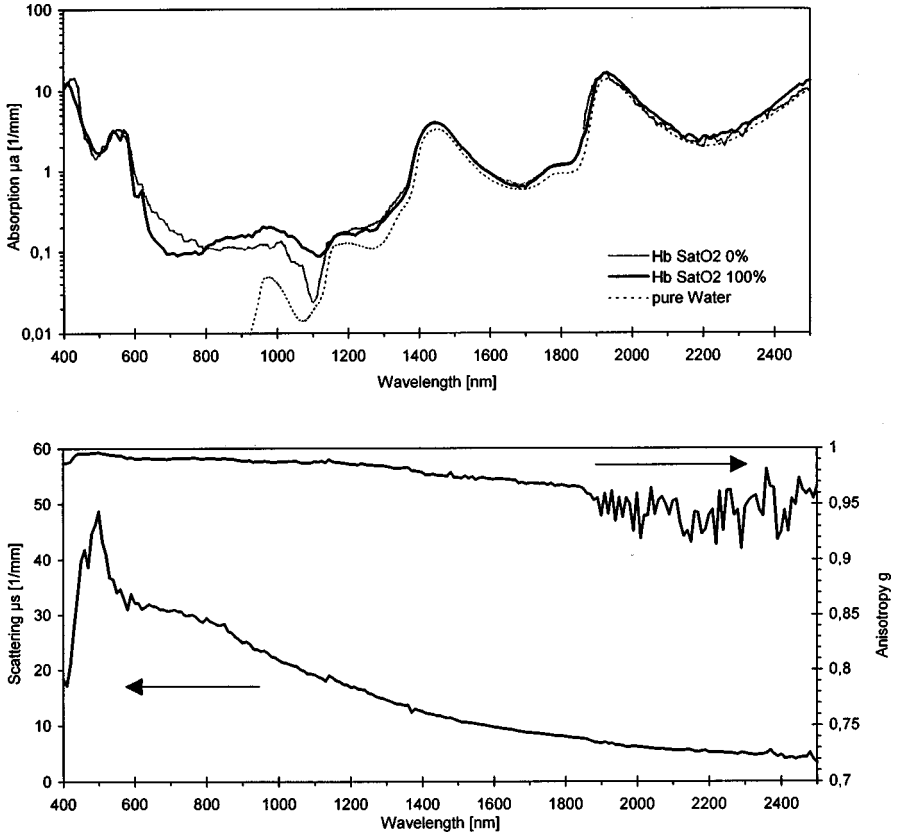

Fig. 13 The absorption spectrum of oxygenated and deoxygenated diluted blood and the values of μ_s and g which did not significantly vary with oxygenation (hct=5%, π=300 mosmol/L, γ=500 s^{-1}).

pected, oxygenation only changed the absorption properties of blood. Scattering remained unaffected by changes in oxygen saturation.

3.6 OPTICAL PROPERTIES OF DILUTED BLOOD IN THE WAVELENGTH RANGE 400–2500 NM

To obtain a complete optical spectrum of blood, measurements in the wavelengths range 400–2500 nm were conducted in increments of $\Delta\lambda = 10$ nm. Figure 13 shows the mean values ($n=3$) of μ_a, μ_s, and g for oxygenated isotonic blood at hct=5% and a shear rate of 500 s^{-1}. In addition, the measurements were repeated for completely deoxygenated blood samples. Significant differences were only found for the absorption coefficient in the wavelength range of 400–1200 nm. Here the spectra correlated qualitatively with literature data on haemoglobin solutions.[22–24] The absorption spectra showed the well-known characteristic maximums around 420 and 540 nm and the isosbestic point at 805 nm. However, μ_a was approximately twice the reported haemoglobin solutions if they were scaled to our measured concentration of 18 g/L (hct =5%). Above 1200 nm the absorption spectra of oxygenated and deoxygenated blood were not significantly different and followed the water absorption. In the range of 1170 to 1350 nm blood absorption was approximately twice that of water, above 1350 nm μ_a followed the water absorption on a level of approximately 120%–130%. Thus the same effect of increased absorption that was found in the visible region also appeared for the water absorption in the near infrared where other absorbers were negligible. This might also be the result of the internal photon reflection, because it does not matter whether absorption within a scatterer is caused by water or haemoglobin.

In contrast to the absorption coefficient no significant differences between scattering coefficients or anisotropy factors were found for both oxygen saturations over the whole measured wavelength range. The scattering coefficient μ_s showed a distinct maximum at 500 nm with values over 40 mm^{-1} which was consistent with theoretical investigations of Pittman.[26] In the wavelength range 550–800 nm μ_s slightly decreased to values of 30 mm^{-1}. Above 800 nm μ_s decreased proportionally with wavelength to $\lambda^{-1.7}$. At 2500 nm μ_s amounted to 10% of the value found at 500 nm. The decrease of μ_s with wavelength was due to a reduction of the scattering cross section and was consistent with Mie calculations. Considering the measured dilution of the investigated blood sample (hct=5%)

very high scattering coefficients above 350 mm^{-1} at 500 nm can be expected for blood with physiological RBC concentrations (hct≈41%). The anisotropy factor g was larger than 0.98 in a wavelength range from 400 to 1400 nm with maximum values over 0.99 in the range 400 to 600 nm. Above 1400 nm g decreased slightly to values about 0.95 in the near infrared. The increasing oscillation of g above 1800 nm was caused by the small values of the measured quantities. Especially R_d was found to be far below 0.1% in this range. These results confirm the forward scattering characteristic of blood over a wide range of wavelength.

4 SUMMARY AND CONCLUSION

Fundamental knowledge about the optical behavior of human blood could be derived in the present study. We found that measurements under flow conditions were a necessary prerequisite to get exact and reproducible results on blood samples. The double integrating sphere technique proved to be a reliable method to determine macroscopic optical properties. It was necessary to apply inverse Monte Carlo simulations that took into consideration all kinds of systematic errors to calculate precise intrinsic optical properties from the measured quantities. One of the most important details was the application of an optimized scattering phase function for red blood cells. We found that the Gegenbauer–Kernel phase function with $\alpha_{GK}=1$ fit best to the scattering behavior of blood samples. The impact of variations of the most important physiological blood parameters on the optical properties was measured at 632.8 nm using a HeNe laser. We found that

1. Scattering and absorption increased linearly with haematocrit if hct<50%.
2. Absorption and scattering decreased slightly with increasing shear rate.
3. Axial migration was the predominant factor on the optical properties with respect to the flow parameters.
4. The deformation of erythrocytes had no significant impact on the optical properties if volume and haemoglobin content was kept constant.
5. Increasing osmolarity lead to an increase of absorption while scattering and anisotropy decreased.
6. Mie calculations on spherical equivalents provided a precise estimation of the RBC scattering behavior.
7. Increasing haemolysis led to a reduction in absorption and scattering.
8. Haemoglobin solutions had a smaller absorption coefficient than whole blood at the same haemoglobin concentration.
9. The membranes of red blood cells had only a minor impact on the scattering behavior.
10. Oxygenation only changed the absorption properties.

The spectral overview in the wavelength range 400–2500 nm at hct=5% lead to the following conclusions:

1. Blood absorption followed haemoglobin absorption in the range 400–1200 nm on a level of approx. 200%.
2. Blood absorption followed water absorption at wavelength above 1200 nm on a level of 120% to 200%.
3. A distinct difference between oxygenated and deoxygenated blood was only found for the absorption coefficient in the range 400–1200 nm.
4. Scattering showed a maximum around 500 nm and decreased with wavelength at a rate of approximately $\lambda^{-1.7}$.
5. Anisotropy was higher than 0.99 in the range 400–800 nm, higher than 0.98 in the range 800–1400 nm and higher than 0.9 between 1400 and 2500 nm.

One can conclude that scattering of blood is mainly caused by a high refractive index of the haemoglobin solution within the RBCs. Internal reflections of photons lead to an increase of the overall absorption coefficient by increasing the optical path length within the cells. This effect explains the difference between normal and haemolysed blood as well as the increase of absorption with increasing osmolarity and the increased water absorption in the near infrared.

The presented data provide the calculation of optical properties of blood for any given haematocrit up to 50% because scattering increases linearly with haematocrit and anisotropy remains unchanged. For the adaptation of the absorption coefficient it is necessary to separate between haemoglobin and water absorption.

REFERENCES

1. A. Ishimaru, *Wave Propagation and Scattering in Random Media*, Vol. 1, Academic, New York (1978).
2. A. Ishimaru, *Wave Propagation and Scattering in Random Media*, Vol. 2, Academic, New York (1978).
3. J. Reichmann, ''Determination of absorption and scattering coefficients for nonhomogenious media 1: Theory,'' *Appl. Opt.* **12**(8), 1811–1815 (1973).
4. A. Roggan, O. Minet, C. Schroeder, and G. Mueller, ''Measurements of optical properties of tissue using integrating sphere technique. SPIE Institute for Advanced Optical Technologies,'' in *Medical Optical Tomography: Functional Imaging and Monitoring*, G. Müller et al., Eds., Vol. IS11, pp. 149–165, SPIE Press, Bellingham, WA (1993).
5. A. Roggan, K. Dörschel, O. Minet, D. Wolff, and G. Müller, ''The optical properties of biological tissue in the near infrared wavelength range—review and measurements,'' in *Laser-induced Interstitial Thermotherapy*, G. Müller and A. Roggan, Eds., pp. 10–44, SPIE Press, Bellingham, WA (1995).

6. A. Roggan, ''Dosimetrie thermischer Laseranwendungen in der Medizin—Untersuchung der optischen Gewebeeigenschaften und mathematisch-physikalische Modellbildung,'' PhD Dissertation, Technische Universität Berlin, in *Fortschritte in der Lasermedizin*, G. Müller and H.-P. Berlien, Eds., Vol. 16, Ecomed, Landsberg (1997).
7. P. Kubelka and F. Munk, ''Ein Beitrag zur Optik der Farbanstriche,'' *Z. Tech. Phys. (Leipzig)* **12**, 593–601 (1931).
8. L. G. Henyey and J. L. Greenstein, ''Diffuse radiation in the galaxy,'' *Astrophys. J.* **93**, 70–83 (1941).
9. H. C. van de Hulst, *Multiple Light Scattering*, Vol. 1, Academic, New York (1980).
10. H. C. van de Hulst, *Multiple Light Scattering*, Vol. 2, Academic, New York (1980).
11. S. T. Flock, B. C. Wilson, and M. S. Patterson, ''Total attenuation coefficients and scattering phase functions of tissue and phantom materials at 633 nm,'' *Med. Phys.* **14**(4), 835–841 (1987).
12. S. L. Jacques, C. A. Alter, and S. A. Prahl, ''Angular dependance of HeNe laser light scattering by human dermis,'' *Lasers Life Sci.* **1**(4), 309–333 (1987).
13. M. Arnfield, J. Tulip, and M. McPhee, ''Optical propagation in tissue with anisotropic scattering,'' *IEEE Trans. Biomed. Eng.* **35**, 372–381 (1988).
14. S. Prahl, ''Light Transport in Tissue,'' PhD Dissertation, University of Texas at Austin (1988).
15. R. Marchesini, A. Bertoni, S. Andreola, E. Melloni, and A. E. Sichirollo, ''Extinction and absorption coefficients and scattering phase functions of human tissues in vitro,'' *Appl. Opt.* **28**(12), 2318–2324 (1989).
16. M. J. C. van Gemert, S. L. Jacques, H. J. C. M. Sterenborg, and W. M. Star, ''Skin optics,'' *IEEE Trans. Biomed. Eng.* **36**, 1146–1154 (1989).
17. M. Essenpreis, P. van der Zee, P. S. Jones, P. Gewehr, and T. N. Mills, ''Changes in scattering phase function of rat liver at 1.064 μm and 1.321 μm following photocoagulation,'' *Lasers Surg. Med.* **11**, Suppl. 3, 5 (1991).
18. A. N. Yaroslavsky, I. V. Yaroslavsky, T. Goldbach, and H. J. Schwarzmaier, ''The optical properties of blood in the near infrared spectral range,'' *Proc. SPIE* **2678**, 314–324 (1996).
19. L. Reynolds, ''Diffuse reflectance from a finite blood medium: applications to the modeling of fiber optic catheters,'' *Appl. Opt.* **15**(9), 2059–2067 (1976).
20. J. R. Zijp and J. J. ten Bosch, ''Pascal program to perform Mie calculations,'' *Opt. Eng.* **32**(7), 1691–1695 (1993).
21. R. A. MacRae, A. McClure, and P. Latimer, ''Spectral transmission and scattering properties of red blood cells,'' *J. Opt. Soc. Am.* **51**(12), 1366–1372 (1961).
22. E. Gordy and L. Drabkin, ''Determination of the oxygen saturation of blood by a simplified technique applicable to standard equipment,'' *J. Biol. Chem.* **227**, 285–299 (1957).
23. J. M. Steinke and A. P. Shepherd, ''Effects of temperature on optical absorbance spectra of oxy-, carboxy-, and deoxyhemoglobin,'' *Clin. Chem.* **38**(7), 1360–1364 (1992).
24. J. T. Kuenstner and K. H. Norris, ''Spectrophotometry of human hemoglobin in the near infrared region from 1000 to 2500 nm,'' *J. Near Infrared Spectrosc.* **2**, 59–65 (1994).
25. J. M. Steinke and A. P. Shepherd, ''Diffusion model of the optical absorbance of whole blood,'' *J. Opt. Soc. Am. A* **5**(6), 813–822 (1988).
26. R. N. Pittman, ''*In vivo* photometric analysis of hemoglobin,'' *Ann. Biomed. Eng.* **14**, 119–137 (1986).